Electronic Supplementary Material (ESI) for Physical Chemistry Chemical Physics.


# Supplementary Materials for

## Prediction of a two-dimensional high Curie temperature Weyl nodal lines Kagome semimetal

Table S1: The energies (eV) of the four magnetic configurations at the different $U$ ($U_{eff}$ = 0-8 eV) values.

| | **AFM1** | **AFM2** | **AFM3** | **FM** |
|---|---|---|---|---|
| **$U_{eff}$ = 0** | **-113.8263** | **-112.9044** | **-113.7001** | **-114.2936** |
| **$U_{eff}$ = 1** | **-106.7243** | **-105.2586** | **-106.3794** | **-107.6227** |
| **$U_{eff}$ = 2** | **-100.0409** | **-98.6580** | **-99.5270** | **-101.2309** |
| **$U_{eff}$ = 3** | **-93.7284** | **-92.7104** | **-93.0807** | **-95.1184** |
| **$U_{eff}$ = 4** | **-87.7632** | **-87.1342** | **-87.1003** | **-89.2828** |
| **$U_{eff}$ = 5** | **-82.2687** | **-81.8912** | **-81.5391** | **-83.7197** |
| **$U_{eff}$ = 6** | **-77.0445** | **-76.9540** | **-76.3351** | **-78.4241** |
| **$U_{eff}$ = 7** | **-72.1087** | **-72.3010** | **-71.5133** | **-73.3911** |
| **$U_{eff}$ = 8** | **-67.5010** | **-67.9149** | **-67.5745** | **-68.6166** |

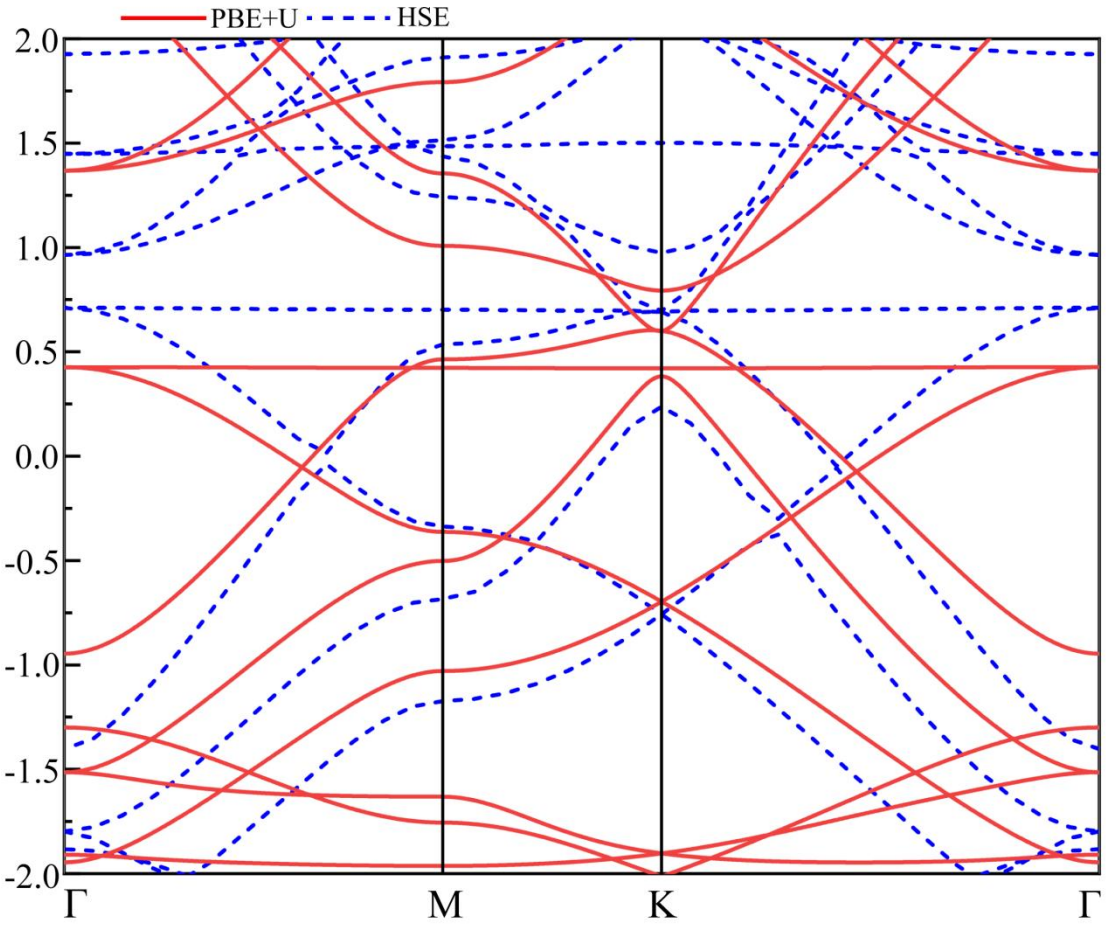


Fig. S1 Band structures for $Mo_2Se_3$ by PBE + *U* and HSE method.

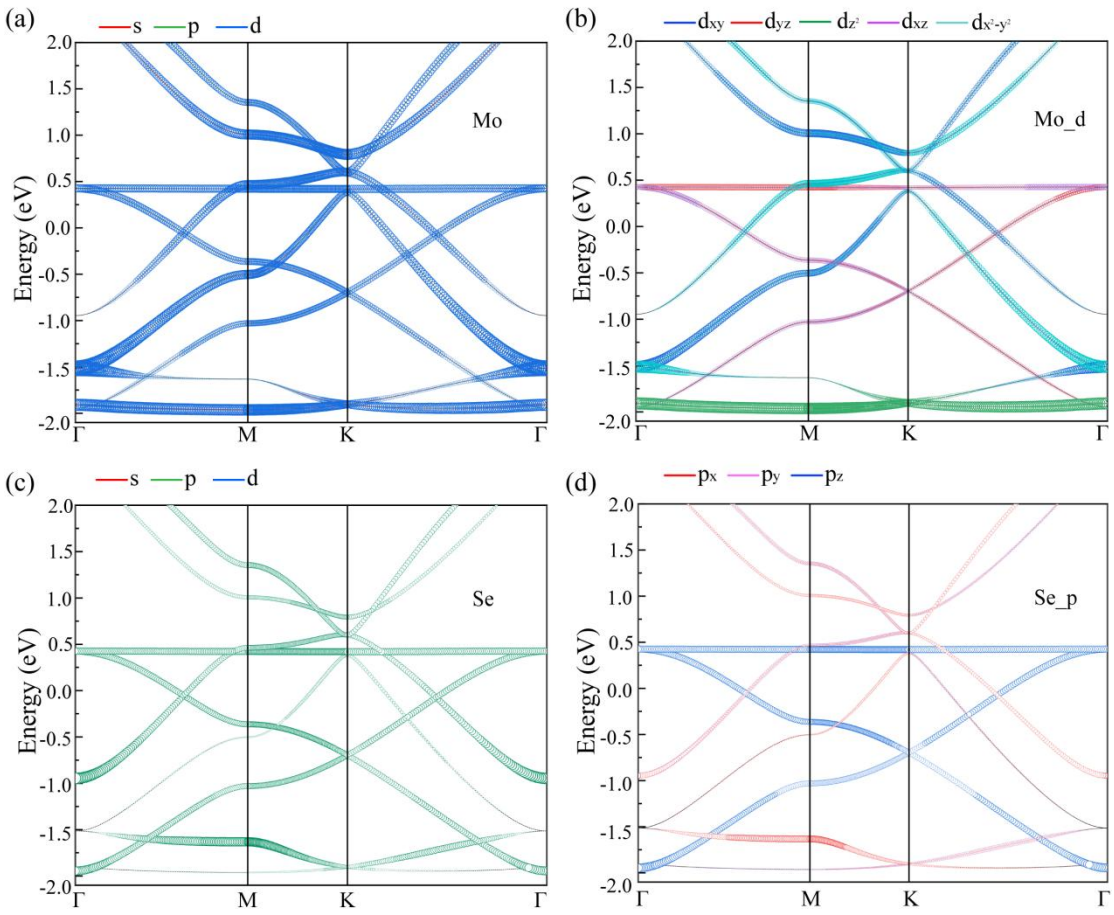


Fig. S2 Contribution of splitting orbitals to the band structures of monolayer $Mo_2Se_3$ at the PBE + *U* level without considering SOC effects. The color intensity shows the amplitude of the orbital-resolved character.

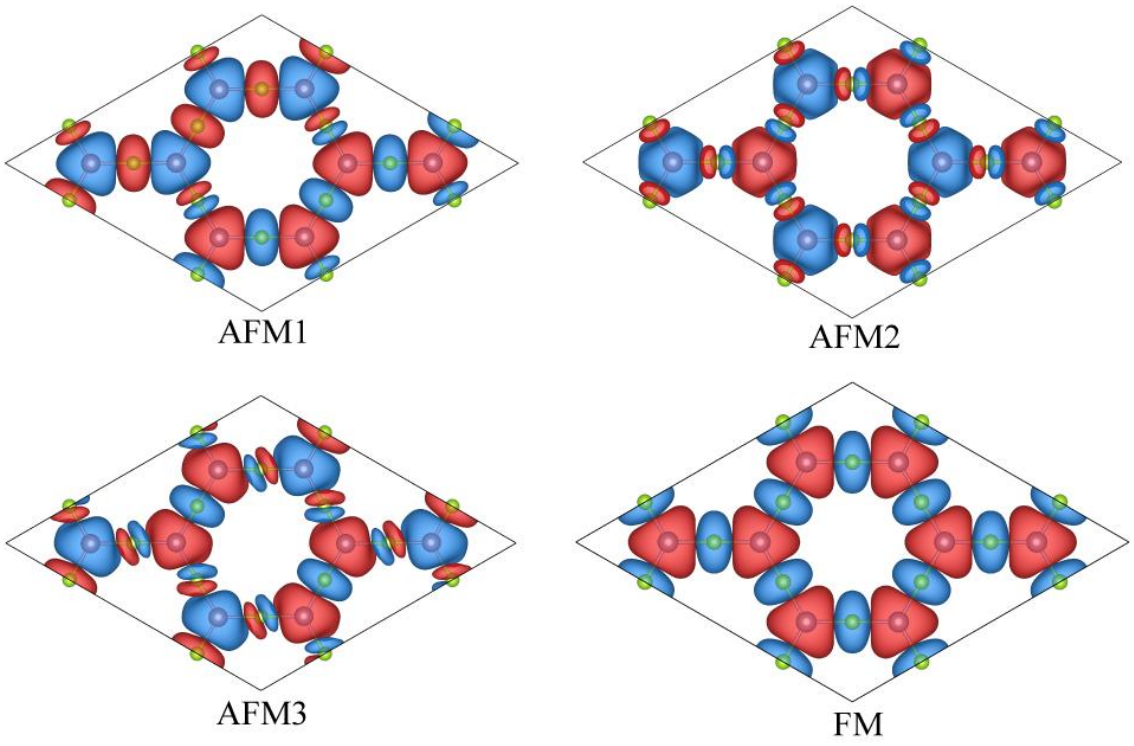


Fig. S3 Spatial spin density distribution of $Mo_2Se_3$ monolayer for the different magnetic configurations in a 2 × 2 × 1 supercell with the isosurface value set as 0.0008 *e*/Bohr$^3$. The red and blue colors refer to the spin-up and spin-down densities, respectively.

Table S2: Total and atomic magnetic moments of $Mo_2Se_3$ monolayer obtained from OUTCAR of VASP.

| | Total magnetic moment ($\mu_B$) | Atomic magnetic moment (AMM) ($\mu_B$) | (AMM) ($\mu_B$) |
|---|---|---|---|
| $Mo_2Se_3$ | 5.266 | Mo : 3.048 | Se : -0.277 |

Table S3: The squared difference between the elements of the orbital angular momentum matrix for spin-up *d* orbitals in both magnetization directions ($\left|\langle o^+|L_x|u^+\rangle\right|^2 - \left|\langle o^+|L_z|u^+\rangle\right|^2$).

| | $o^+$ | | | | |
|---|---|---|---|---|---|
| $u^+$ | $d_{xy}$ | $d_{yz}$ | $d_{z2}$ | $d_{xz}$ | $d_{x2-y2}$ |
| $d_{xy}$ | 0 | 0 | 0 | -1 | 4 |
| $d_{yz}$ | 0 | 0 | -3 | 1 | -1 |
| $d_{z2}$ | 0 | -3 | 0 | 0 | 0 |
| $d_{xz}$ | -1 | 1 | 0 | 0 | 0 |
| $d_{x2-y2}$ | 4 | -1 | 0 | 0 | 0 |

Table S4: The squared difference between the elements of the orbital angular momentum matrix for spin-up *p* orbitals in both magnetization directions ($\left|\langle o^+|L_x|u^+\rangle\right|^2 - \left|\langle o^+|L_z|u^+\rangle\right|^2$).

| | $o^+$ | | |
|---|---|---|---|
| $u^+$ | $p_y$ | $p_z$ | $p_x$ |
| $p_y$ | 0 | -1 | 1 |
| $p_z$ | -1 | 0 | 0 |
| $p_x$ | 1 | 0 | 0 |

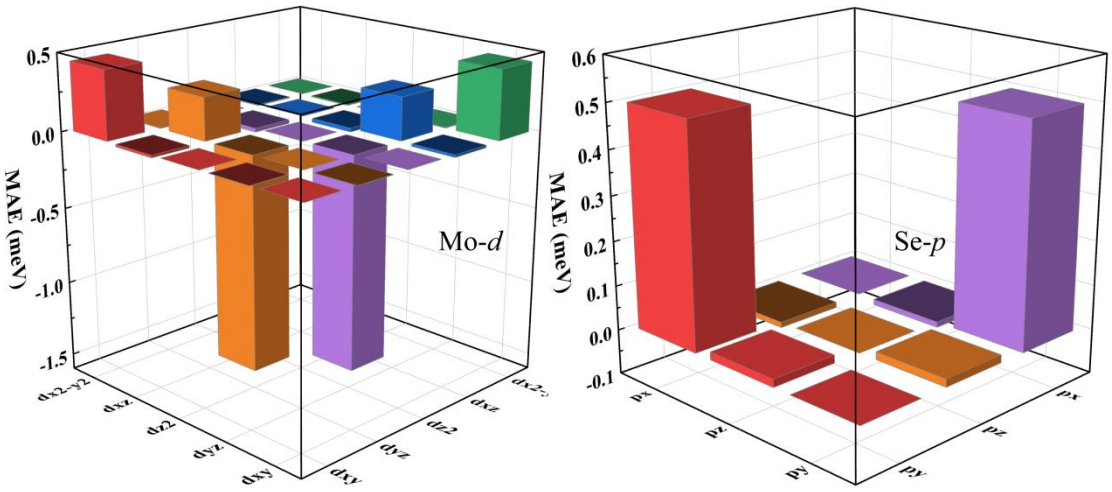


Fig. S4 The Mo-*d* and Se-*p* orbital-resolved MAEs of the $Mo_2Se_3$ monolayer.

The method of obtaining Heisenberg magnetic exchange constant by first principles calculations is shown below. With spins pointing in the *x*, *y*, and *z* directions, the energy expressions are:

$$E_i^{x(y)} = E_0 + \frac{S^2}{2}\sum_d N_i(d) J_{x(y)}(d)$$

$$E_i^z = E_0 + NAS^2 + \frac{S^2}{2}\sum_d N_i(d) J_z(d)$$

$$A = \frac{E_{FM}^z - E_{FM}^x}{2|S|^2}$$

$E_i^{x(y)}$ and $E_i^z$ are the energy of PBE + $U$ + SOC calculation along the *x*(*y*) and *z* axis, respectively. $N_i(d) = N_{\mathrm{FM}}^i(d) - N_{\mathrm{AFM}}^i(d)$ is the difference between the number of the *d*th nearest neighbor (*d*NN) FM bonds and the AFM bonds, $J(d) = \left[J_x(d) + J_y(d)\right]/2$ and $\lambda(d) = J_z(d) - J(d)$.

After algebra, we can obtain all the parameters listed in the table

(a) (b)

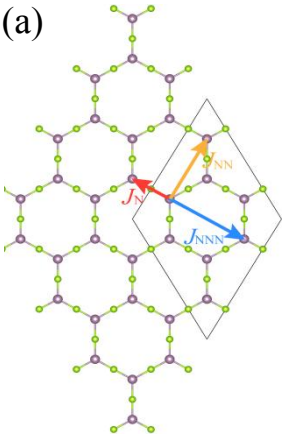


| | N | NN | NNN |
|---|---|---|---|
| $J_{xx}(J_{yy})$ (meV) | 39.40 | 10.74 | 0.92 |
| $J_{zz}$ (meV) | 39.07 | 10.67 | 0.87 |
| $\lambda$ (meV) | -0.33 | -0.08 | -0.05 |
| A = 1.06 meV | | | |

Fig. S5 (a) Top view showing the nearest (N), next-nearest (NN), and next-next-nearest (NNN) exchange-coupling parameters $J_N$, $J_{NN}$, and $J_{NNN}$ for the $Mo_2Se_3$ monolayer. (b) Exchange coupling parameters and single-ion magnetic anisotropy parameter for the 2 × 2 × 1 supercell.

The Monte Carlo simulations are carried out using the Metropolis algorithm based on the classical Heisenberg model, and the specific heat capacity is calculated using the dissipation-fluctuation theorem. During the MC simulations, a 40 × 40 supercell is used to minimize the periodic boundary conditions. At each temperature, the spins of all magnetic points are flipped randomly. 30000 scans are performed to fully thermalize the system to equilibrium, and all statistical results are obtained from the next 60000 scans. All of these are implemented in the MCSOLVER.

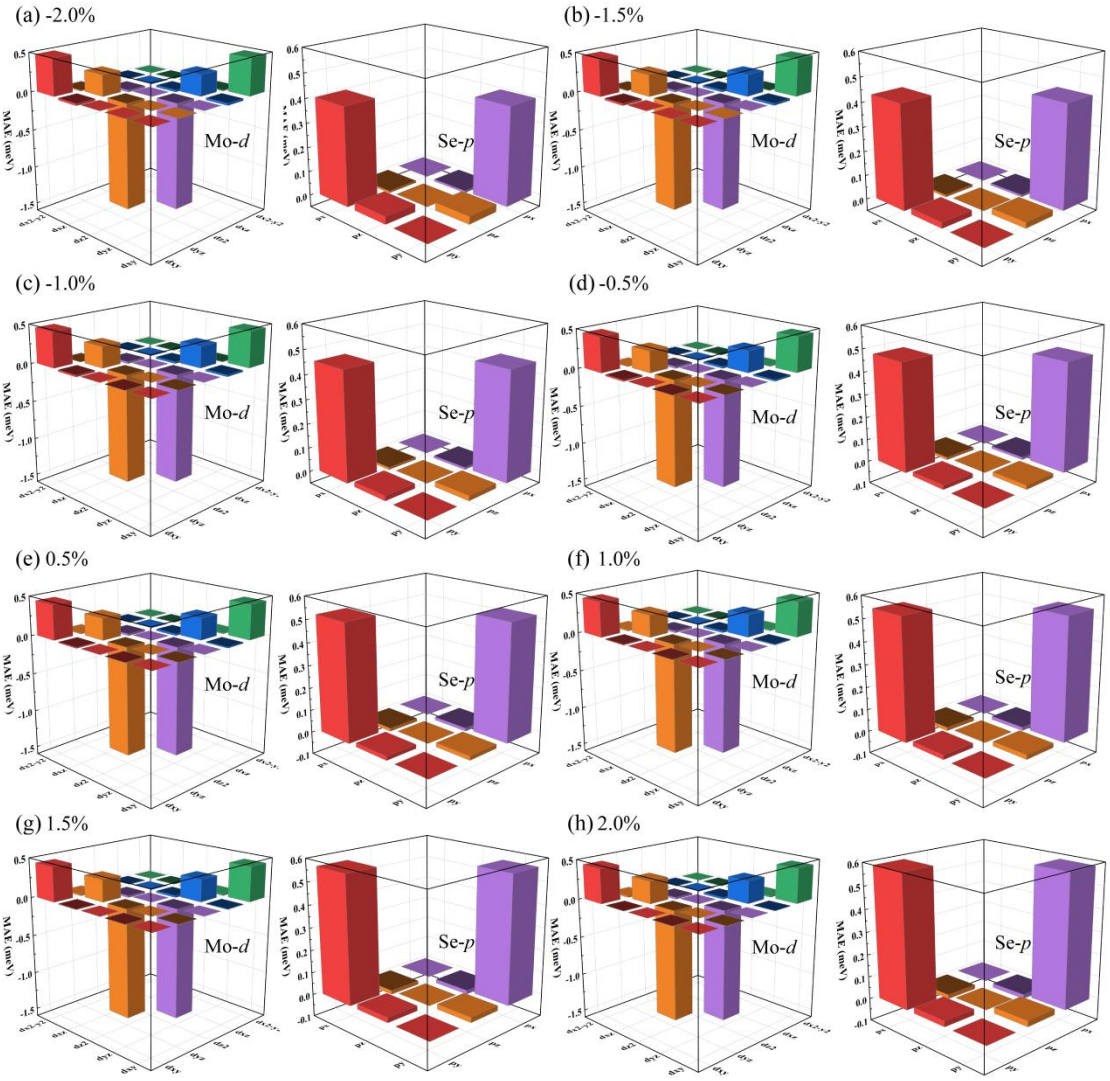


Fig. S6 The Mo-*d* and Se-*p* orbital-resolved MAEs of the $Mo_2Se_3$ monolayer under different strains.

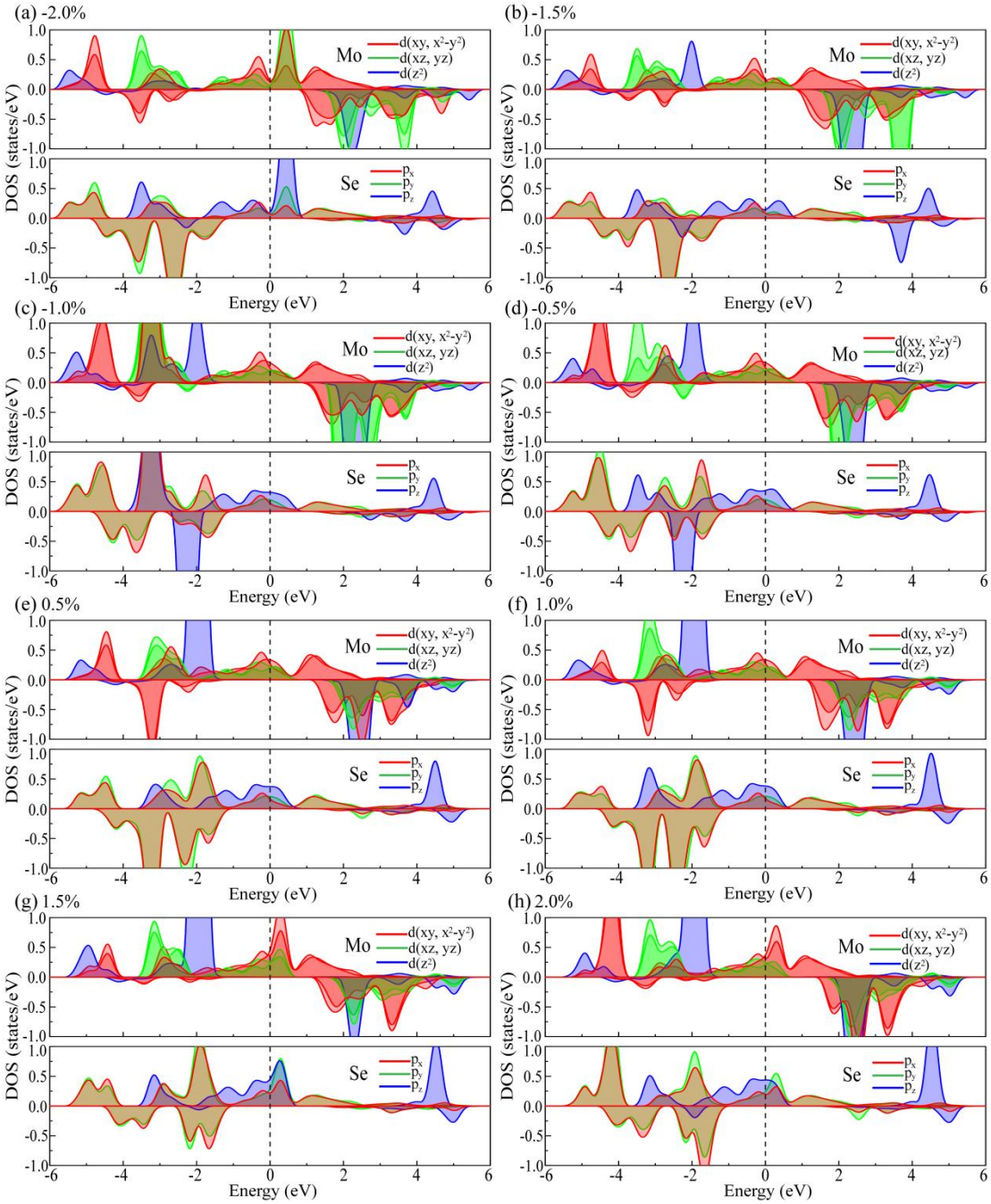


Fig. S7 The projected density of states of Mo-*d* and Se-*p* orbitals of $Mo_2Se_3$ monolayer under different strains.